LO-09-022

Experimental Investigation of the Effect of Various Parameters on the Infiltration Rates of Single Band Open Vertical Refrigerated Display Cases with Zero Back Panel Flow

Mazyar Amin **Dana Dabiri, PhD** **Homayun K. Navaz, PhD**
Member ASHRAE

ABSTRACT

Open Refrigerated Vertical Display Cases greatly contribute to the energy consumption of supermarkets. In the recent decades air curtains have significantly improved the efficiency of the systems; nevertheless, it is possible to change the design specifications of display cases to achieve higher degrees of efficiency. A simulator apparatus was constructed to easily vary several geometrical and fluid dynamic variables that affect the air curtain performances, and then a series of experimental tests were performed by a noble tracer gas technique to measure the infiltration rate in each test case scenario. The study focuses only on the cases that do not benefit from back panel flow and therefore the ratio is 1. In addition to the infiltration rate measurement, a new method using tracer gas is used to measure the total flow rate of the display case. It was found that the infiltration rate is strongly dependent on the investigated variables.

INTRODUCTION

In supermarkets, Open Refrigerated Vertical Display Cases (ORVDC) are commonly used to store and maintain food products at prescribed temperatures. A large number of such systems are constructed without doors (Figure 1a) allowing easy access to the food products.

These systems also prevent the fogging problem that occurs on the interior side of the glass of the refrigerators with doors. As a result, a lot of ambient air laden with higher contents of energy than the cold air within the system, can penetrate onto the shelves of the system and undesirably increase the temperature of the food products. When this occurs, the temperature sensors placed close to the food products operate the compressor until the lower prescribed temperature is attained. In 2003, a study by California Energy Commission, and Southern California Edison Co. estimated that about 70,000 ORVDCs were operating in the supermarkets of the United States. The projected energy consumption associated with these systems was a tremendous amount, about 1,000 GW-hr (3.4×10^{12} Btu/hr) per year. In several studies such as the work of Howell and Adams (1991), up to 80% of the cooling load of the systems were attributed to the infiltrated warm air. It is also estimated that up to 50% of the total energy costs of supermarkets is due to the operation of the display cases. Thus, one may conclude that the source of up to 40% of the total energy costs of a supermarket is from entrainment of room air by ORVDCs, which will end up with 400 GW-hr (1.37×10^{12} Btu/hr) per year. Given the enormous amount of energy, designing the systems with a more efficient air curtain is crucial. Efficiency of the systems can be partially characterized by the amount of infiltrated mass. In the first step, this mass should be measured accurately, which is done by tracer gas in this study.

In HVAC applications tracer gases are used to measure the infiltration or leakage of air between the interior and exterior of a building. Losses can occur through closed windows and doors or any other holes and cracks in the building construction. In the same fashion, tracer gases are applicable in measuring the leakage from air distribution units. Moreover, effectiveness of a ventilation system in distributing air within a room or zone can be evaluated by releasing a tracer gas and tracking it spatially and temporally. A review on the tracer gas techniques in HVAC applications can be found in the work of McWilliams (2002).

Amin et al. (2008a) and Faramarzi et al. (2008), for the first time analytically and experimentally tailored the tracer

Mazyar Amin is a PhD candidate and **Dana Dabiri** is an assistant professor in the Aeronautics and Astronautics Department, University of Washington, Seattle, WA. **Homayun K. Navaz** is a professor in the Mechanical Engineering Department, Kettering University, Flint, MI.

gas application to the flow rate measurement of infiltrated air into the display case, as well as measured the operating flow rate of the system. In addition, they demonstrated that the *entrained* air and *infiltrated* air are not essentially identical since not all the entrained air can infiltrate into the RAG (Return Air Grille) and/or onto the shelves after the initial mixing in the air curtain. In this approach they showed (Equation 1) that the amount of infiltrated air is directly proportional to the total flow rate of the display case, i.e. the flow rate through the RAG (Figure 1b). It is also a function of concentrations of the tracer gas at the RAG, Discharge Air Grille (DAG), and the entrained ambient air. Therefore, an accurate measurement of the infiltration is contingent to the accuracy of total flow rate measurement at the RAG.

$$\dot{m}_{Inf} = \dot{m}_{RAG}\frac{C_{DAG} - C_{RAG}}{C_{DAG} - C_{Amb}} \quad (1)$$

This flow rate is also referred to as *absolute* infiltration rate.

A similar temperature-based relationship (Equation 2) has been previously proposed by Rigot (1990) and Navaz et al. (2005b).

$$\dot{m}_{Inf} = \dot{m}_{RAG}\frac{T_{DAG} - T_{RAG}}{T_{DAG} - T_{Amb}} \quad (2)$$

The thermal method (Equation 2) has in fact several disadvantages over the tracer gas technique. Firstly, many numerical and experimental studies such as the work of Navaz et al. (2002, 2005b), and Faramarzi et al. (2008) have shown that the velocity profiles in the DAG and RAG are not necessarily uniform; so, the average temperatures that will be used in this equation must be measured with good resolution in the cross section and must be mass-weighted average quantities. Therefore, an auxiliary experimental method is required for the velocity measurements. Secondly, the velocity measurements should be performed with good resolution across the width (small dimension) of the DAG and RAG to result in accurate average temperature. Also, during the measurements the variations in the total flow rate of the display case during and between frosting and defrosting stages in a full cycle of refrigeration should be taken into account. Some conventional velocity measurement techniques such as Hot-Wire Anemometry (HWA) and Pitot-tube velocimetry, although not as expensive, are not very practical in such an application since they cannot provide the required accuracy and resolution when several of them compacted in a narrow cross section area along the smaller dimension. For example, there is a slight variation in the velocity profile at different longitudinal sections (in z-direction shown in Figure 2) of a display case due to imperfections in design and also presence of wires, etc. Tracer gas method, samples from the flow at least at three different longitudinal sections and at each section the samples are drawn by probes that have several holes on them. This creates better averaging along across the DAG or RAG widths. Insertion of the probes is done neatly, which causes the least possible flow distraction during the operation of the system. In HWA, however, for an accurate measurement, several measurements should be done at each section, which may require insertion of several hot wires. This is in addition to the difficulty associated with insertion of hot-wire within at sections of the duct that should be distant from the inlet or discharge of the duct and are not easily accessible.

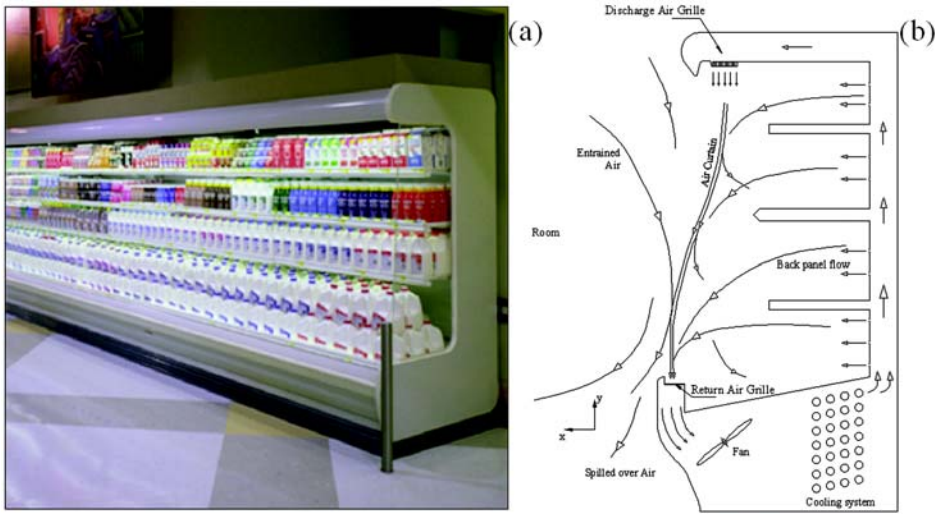

Figure 1 *(a) A typical vertical ORVDC (courtesy of Hill Phoenix Co.) and (b) schematic of side view with flow streamlines.*

In the tracer gas technique, the concentration of the tracer gas can be sampled simultaneously and continuously at several points along the lengths of the zones, DAG and RAG. Then at each zone the concentrations are averaged along the length, resulting in a more accurate, practical, engineering flow rate and infiltration rate. This technique does not require any knowledge about the cross-section area of the measurement region but a good mixing between tracer gas and air is essential.

The laser based visualization techniques, such as Particle Image Velocimetry (PIV) or Laser Doppler Velocimetry (LDV) are more accurate but are time-consuming, cumbersome and cannot keep up with the pace of infiltration data collection. Thirdly, in cases that buoyancy effect is negligible (small Richardson numbers), the systems can be tested under isothermal condition. As a result, Equation 2 is not applicable, but tracer gas can be conveniently used. Fourthly, this equation, does not take into consideration the effect of humidity and humidity ratio, and it is more suited for a dry air. Nonetheless, the comparison between the infiltration rate of tracer gas and the thermal method (Amin et al., 2008a) has pointed out a difference of up to 7% with the former method taking larger values (with identical m_{RAG} in Equations 1 & 2).

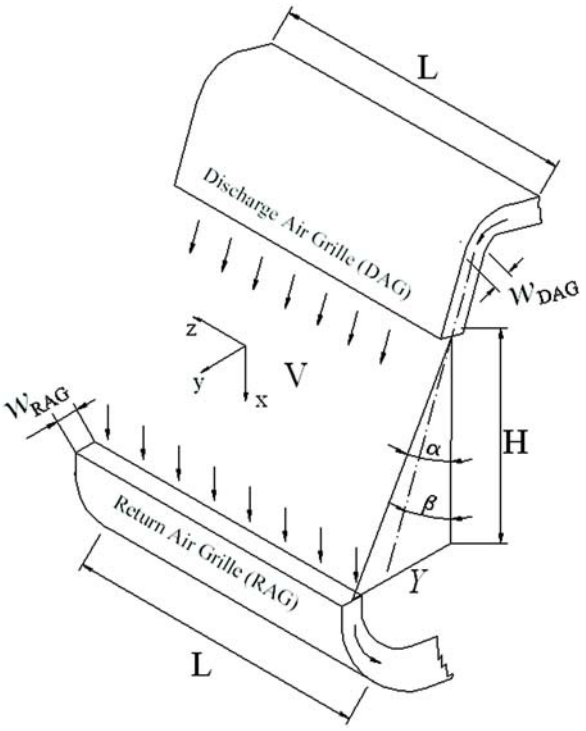

Figure 2 *Schematic of relative geometrical positions of DAG and RAG.*

Investigating the effect of several variables that are thought to be influential to the infiltration is the matter of another discussion in the present work. The non-dimensional form of the variables have been explained in more details in the work of Navaz et al. (2005a) and Amin et al. (2008b), and are summarized In Equation 3.

$$\frac{\dot{m}_{Inf}}{\dot{m}_{tot}} = f\left(\frac{H}{w_{DAG}}, \alpha, \beta, \mathrm{Re}, \frac{\dot{m}_{DAG}}{\dot{m}_{tot}}\right) \quad (3)$$

$$\dot{m}_{tot} = \dot{m}_{RAG} = \dot{m}_{BP} + \dot{m}_{DAG} \quad (4)$$

The term on the left side of the equation represents the ratio of infiltrated air from the ambient side to the total operating flow rate of the display case. The first three variables in the parenthesis have been illustrated in Figure 2; Re is the Reynolds number based on the average velocity of the DAG and width of the DAG as its characteristics length. The last term on the right side accounts for the ratio of flow discharged from the DAG to the total operating flow rate. This study only focuses on the cases where the flow rate through the DAG and RAG are the same, i.e. the last term is one.

Overall, this work attempts to present and discuss the results of tracer gas technique used for measuring the mass flow rate and infiltration flow rate of open display cases that lack the flow from the back side. However, even if zero back panel is not popular, the authors after several studies (including future works on non-zero back panels) would like to show why and under what circumstances zero back panel flow is not very popular. However, this judgment is put off for after completing the future studies.

PROBLEM DESCRIPTION

The main goal of the current work is to experimentally investigate the dependency of the infiltration rate on variables on the right side of Equation 3. In order to investigate the effect of the variables with the minimum resolution to form infiltration vs. variable curves, each variable should take at least three values, resulting a total number of 243 tests for all the permutations. Obviously, constructing one display case to accommodate each geometrical configuration is not feasible and requires multitudes of display cases that may cost hundreds of thousands of dollars. Therefore, to alter each variable, a modular, versatile, flexible experimental equipment referred to as the Proof-Of-Concept Air Curtain (POCAC), or simulator, was designed and constructed for conducting the infiltration and mass flow rate tests by tracer gas. An injection system to release the tracer gas, and a sampling and analyzing system to measure the amount of tracer gas concentration at each desired location were employed.

Simulator Apparatus

Figure 3 depicts the simulator. This simulator is a system by which all the variables in Equation 3 can be easily varied. The system excludes a refrigeration system

as it was previously indicated by some researchers such as Navaz et al. (2002) and Faramarzi et al. (2008) that at the range of Reynolds numbers, which are typical in this application, the difference between the DAG and ambient temperatures is not very significant and determinative to the amount of infiltrated air. In typical display cases the air curtain is momentum-driven and buoyancy has negligible effect. Nevertheless, one may anticipate that at smaller Reynolds numbers the effect of Buoyancy plays more important role in the entrainment. In the tracer gas technique, the measurement is based on the change in the concentration of tracer gas from the DAG to RAG; thus it is not required to have information about the thermal quantities and relative humidity.

A wooden *Display Case Prototype* was inserted adjacent to the DAG and RAG to mimic an actual display case. The prototype consists of four shelves, which are fixed, horizontal (i.e. with no tilt angle) and equally distanced. The simulator creates a velocity profile close to a uniform distribution with relatively low turbulence intensity (~ 2.5% to 3%) at the discharge point. To obtain a closer velocity profile to a uniform one with low turbulence intensity at the DAG, the design of the simulator was inspired by the principles of wind tunnel design.

The simulator consists of several air manipulators to improve the uniformity of the flow (especially to improve the homogeneity of the tracer gas in the air flow within the passages of the simulator), and to reduce the turbulence and agitation in the flow. The length of the duct in the upstream of the DAG is sufficiently long and the DAG is distant from the last bend (bend #2) in order to insert several air manipulators to eventually reduce the turbulence at the DAG discharge. Within the simulator there are 6 perforated plates, 2 sets of turning blades, 5 fine screens, and 3 honeycombs. Immediately at the upstream of the DAG, a contraction nozzle assists further attenuating the turbulence. Variation of the height of the opening is made possible by a neoprene bellows; due to the flexibility of the bellows it can provide the desired throw angle (β) as well. Similarly, the horizontal movement is made by another bellows in the lower part of the apparatus. The expansion-to-contraction ratio of the bellows is about 10-to-1. The flow is supplied by a crossflow fan that spans almost the entire length of the simulator; this can give more uniformity to the flow in z-direction than the popular axial fans. The highest point of the system from the floor is 118.1 in. (3 m), the maximum and minimum widths of the simulator in y-direction are 108.7 in. (2.76 m) and 82.3 in. (2.09 m), respectively, and the length of the system in z-direction is 46 in. (1.17m). The opening height (the

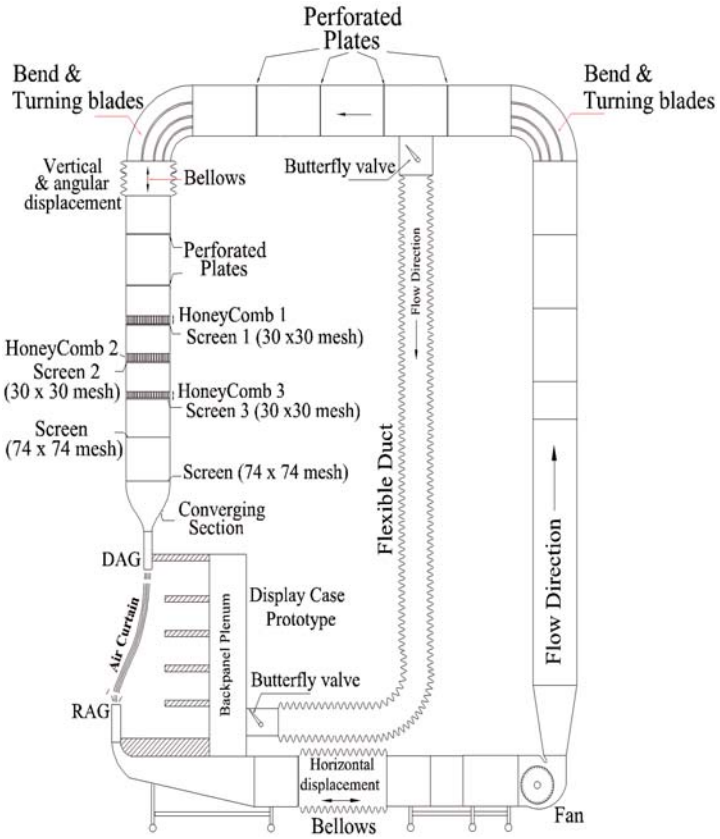

Figure 3 *Side view of the simulator.*

vertical distance between the DAG and RAG) can vary between 2.75 in. (0.07 m) to a maximum of 26 in. (0.66 m). The widths and lengths of both DAG and RAG are identical and equal to 1.6 in. (0.0406 m) and 45 in. (1.143 m), respectively.

It should be mentioned that since non-dimensional variables are used in this study, the non-dimensionalized results of the work can be generalized for any real display case that its non-dimensional variables falls within the range of the current study. However, the dimensions of the simulator were optionally chosen to be the half of the size of a typical display case manufactured by Hill Phoenix Co. To supply flow from the back of the panel and parallel to the shelves, three round flexible ducts were connected to transfer the flow from the upper duct of the simulator to the back panel plenum. It should be noted that the branch location must be somewhere in the downstream of the release point of the tracer gas, where a good mixing could have been achieved at that point. On the back panel plenum side, the flexible ducts are connected to the lower half to simulate the slightly greater flow rate from lower holes of the perforated plate in a display case. The portion of the total flow which will be allocated to the back panel flow can be varied by butterfly valves and/or by inline fans which are installed within the flexible ducts. The DAG and RAG were made from transparent Plexiglas to facilitate the velocity profile measurement in the upstream of the discharge and downstream of the return duct by DPIV. For zero back panel flow, the valves were completely shut off.

Studying non-zero flow rate from the perforated back panel is out of the scope of this study but the results will be published in future articles.

Tracer Gas Technique

As mentioned previously, a tracer gas system and a sampling/analyzing system are required to acquire the concentration of the tracer gas at the locations that the Equation 1 prescribes. The detailed information on the infiltration measurement in display cases by tracer gas can be found in the work of Amin et al. (2008a). Figure 4 shows the entire experimental set up for the tracer gas tests. It should be mentioned that in this work Carbon dioxide (CO_2) was used as the tracer gas and its release was continuous in the entire course of the tests. The maximum volumetric concentration set for the tests was about 3% ≡ 30,000 ppm for the DAG, with an average value of 2.5%. This resulted in lower concentrations in the RAG (maximum around 2%), and even smaller volumetric concentrations in the ambient (under 1%). It should be noted that CO_2 is not flammable or hazardous to the environment if the concentration (ambient concentration) that a human is continuously exposed in a few hours is less than 0.5%? 5,000 ppm (ACGIH 1971 and IDLH 2007). The gas has no smell and no taste. A CO_2 gas analyzer by Horiba Co. was utilized (VA-3000) in this study. The Repeatability, Linearity and Zero/Span shift errors of the gas analyzer are, 0.5%, 1%, and 0.5% of the full scale value, respectively; while the sensitivity of the instrument was less than 1%. The resolution of the instrument

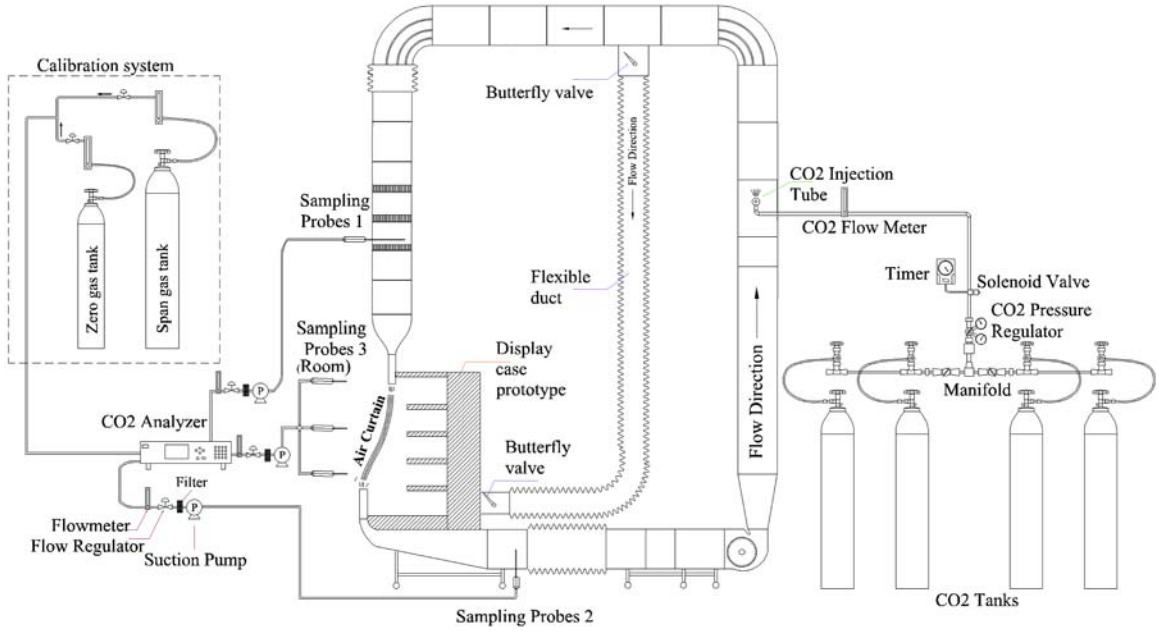

Figure 4 *Simulator with injection and sampling/analyzing systems set up.*

is 1 ppm. The overall uncertainty is about ±480 ppm equivalent to ±1.9% of the full scale value.

Total Flow Rate Analysis

The total mass flow rate of the system can be found by analyzing the mass balance of tracer gas before and after the release point of the gas. The sampling of the tracer gas within the duct should be performed at 1) upstream of the release point 2) upstream of the DAG. The latter should be sufficiently away from the release point to allow a proper mixing prior to sampling. Figure 5 presents the schematic of a confined control volume that extends from point 1 to point 2.

The mass balance of the tracer gas (CO_2 in this work) for the control volume will be:

$$\dot{m}_{CO_2,\,DAG} = \dot{m}_{Inj} + \dot{m}_{CO_2,\,RAG} \tag{5}$$

And the definition of mass concentration at any location is:

$$C = \frac{\dot{m}_{CO_2}}{\dot{m}_{CO_2} + \dot{m}_{air}} \Rightarrow \dot{m}_{CO_2} = \frac{C}{1-C}\dot{m}_{air} \tag{6}$$

By combining Equations 5 and 6 one will get:

$$\frac{C_{DAG}}{1-C_{DAG}}\dot{m}_{air} = \dot{m}_{Inj} + \frac{C_{RAG}}{1-C_{RAG}}\dot{m}_{air} \tag{7}$$

Solving for $\dot{m}_{air}$ (total mass flow rate of air, i.e. mass flow rate through RAG) will yield:

$$\dot{m}_{air} = \frac{\dot{m}_{Inj}}{\left[\frac{C_{DAG}}{1-C_{DAG}} - \frac{C_{RAG}}{1-C_{RAG}}\right]} \tag{8}$$

RESULTS

Table 1 presents the values of the non-dimensional variables in Equation 3 that were tested in this work. These values usually cover a wide range of typical display cases. The tests were conducted for shelves with no food products.

144 different scenarios were tested for the variables of the table. It should be again emphasized that since the variables used in this work are in non-dimensional form, the non-dimensional results can be generalized to any display case system regardless of its size and total flow rate of the system provided that the display case obtains non-dimensional variables that fall within the range of our data points. In this work due to multitudes of the data and plots, it is not possible to present all of them, and only a selection of the data will be rendered. In all cases the turbulence intensities were relatively small and fixed between 2.5% to 3%.

The amount of air supplied by the fans of display cases is one of the variables that has been discussed over its optimum value. Our experimental results show that the *absolute* value of infiltration rate (Equation 1) in all test case scenarios increases with increase of Reynolds number.

Figure 6 depicts change variation of infiltration with of Re in two different cases. In fact the higher speed the jet gets, the higher turbulence will be induced in the downstream of the jet exit. This in turn will enhance entrainment of more ambient air into the air curtain jet and more mixing, and consequently will result in ingress of greater amount of ambient air into the system, which can contain higher content of energy (temperature and humidity).

It is evident from the figure that at smaller Reynolds numbers the difference between the absolute infiltrations of different offset angles (α) will get smaller.

By dividing both sides of Equation 1 by $\dot{m}_{RAG}$, one can obtain:

$$\frac{\dot{m}_{Inf}}{\dot{m}_{RAG}} = \frac{C_{DAG} - C_{RAG}}{C_{DAG} - C_{Amb}} \tag{9}$$

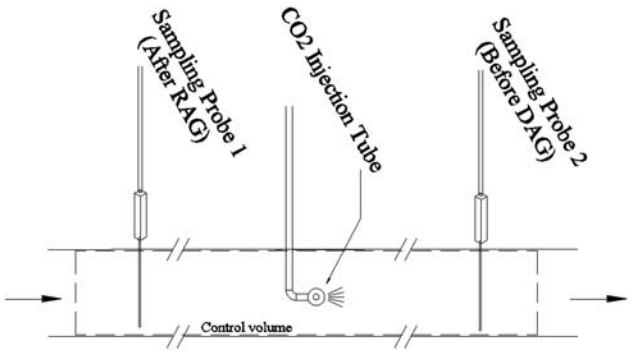

Figure 5 *Control volume inside the simulator duct between two sampling locations.*

Table 1. Values of Nondimensional Variables

$\frac{\dot{m}_{DAG}}{\dot{m}_{tot}}$		1		
H/w	8	12	16	
α	0°	16°	24°	
β	–5°	0°	5°	13°
Re_{DAG}	2200	3400	5500	8400

NOTE: The negative sign in β indicates that the DAG is tilted toward the inside the display case.

This term, which is referred to as Non-dimensional Infiltration Rate or N.I.R. (Amin et al., 2008b), resembles *thermal entrainment* η used by Rigot (1990):

$$\eta = \left| \frac{T_{DAG} - T_{RAG}}{T_{DAG} - T_{Amb}} \right| \quad (10)$$

Figure 7 corresponds to the N.I.R. values of the data in Figure 6.

Comparing the graphs of Figures 6 & 7 reveals that although the absolute infiltration rate increases monotonically with increase of Re, the N.I.R. decreases when Re increases. Such different behaviors may be explained by attributing the N.I.R. to the efficiency of an air curtain in entraining less ambient air. For example, the smaller value of N.I.R. at higher Re number implies that the air curtain tends to entrain and infiltrate *relatively* small amount of the ambient air despite its strong momentum. Furthermore, the absolute infiltration rate changes almost linearly with Re in our entire test range. The N.I.R., however, decreases rapidly with Re when it changes from 2,200 to 3,400, and then after Re=3,400 continues to drop with slower rate and almost linearly. These trends of change of absolute and non-dimensional infiltration rates have been seen in all the test case scenarios of this study. It was also found (not shown here) that at larger throw angles (β), the dependency of both absolute infiltration and N.I.R. on angle α is smaller. This is more pronounced at smaller *H/w* ratios (e.g. *H/w*=8). Moreover, in most scenarios, with increase of α, absolute and non-dimensional infiltration rates increase; this can be seen in Figures 6 & 7 too. This is perhaps due to the larger curvature that an air curtain gains when offset angle increases. The subsequent effects of increasing α on the development of the flow domain around the air curtain can be in the form of partial impingement of the jet on the display case tray (very bottom horizontal surface of the display case), and its upward agitated feedback flow. In most cases, as shown in

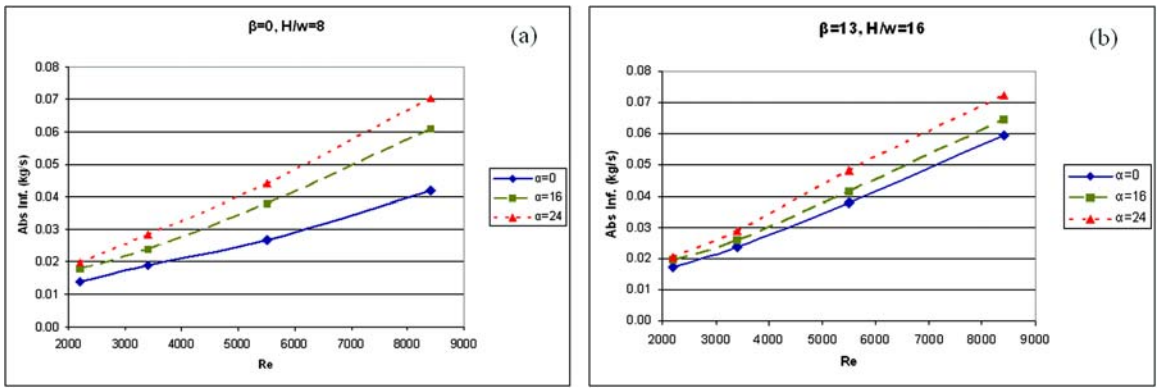

Figure 6 *Effect of Reynolds number of the absolute infiltration.*

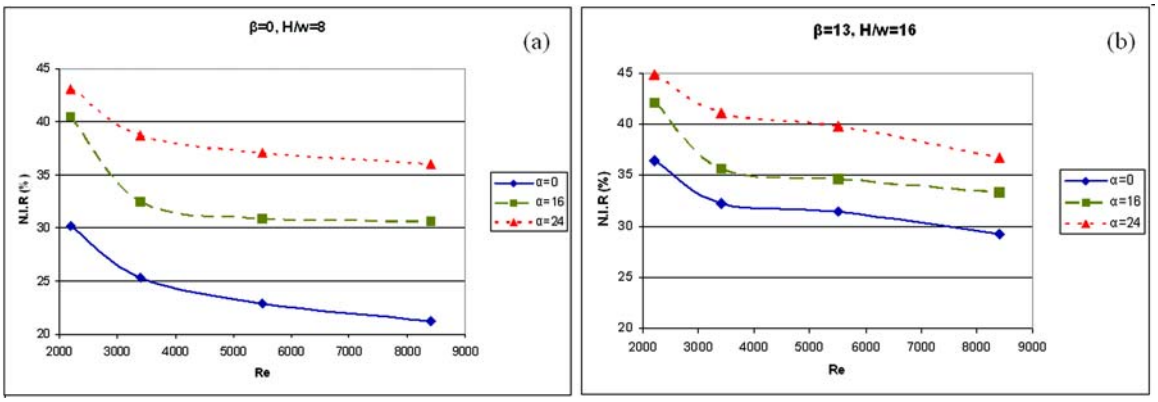

Figure 7 *Effect of Reynolds number on the nondimensional infiltration rate (N.I.R.).*

Figure 8, the dependency of infiltration on α is almost linear particularly at smaller values of α. Between α=16° and 24°, however, some non-linearities were noticed. Similar trends can be seen for N.I.R. (not been presented here).

Figure 8 also shows that infiltration is affected by change of β. Interestingly, the smallest β (i.e. -5°) almost in all cases brings about the least amount of infiltration. Its N.I.R. is characterized by similar behavior too. However, the infiltration rate (both absolute and non-dimensional values) experiences various patterns of change with change of β. As mentioned above, β = -5° always causes the least amount of infiltration amongst the values, but with increases of β from -5° to 0°, usually the infiltration increases and then decreases or stays constant up to β=5°; with further increase of β to greater values than 5°, and depending on the *H/w* ratio, the infiltration may increase, decrease or stay unchanged (Figures 9a & 9b). This variation is more pronounced at the smallest value of *H/w*, i.e. 8. As a matter of fact, at *H/w*=8 when β takes the largest value (i.e., 13°), infiltrations of all α angles converge and the dependency of infiltration on β is lost (Figure 9a). However, no significant change in the pattern of variation of β at fixed α's were seen when Re changed.

Opening height of a display case is another factor that has always and in this study been very influential to the amount of infiltration and one may expect that with change of H the curvature of the air curtain that is also function of α and β, change again. The results show that with change of *H/w* various patterns of change were found for the infiltration rate. For instance in Figure 10a, where β=-5° and Re=2,200, the infiltration rate experiences a minima at around *H/w*=12. If β=-5° and Re=5,500 (Figure 10b) the infiltration increases monotonically with increase of *H/w*. That is,

$$\frac{d(Inf)}{d\left(\frac{H}{w}\right)} > 0, \quad \frac{d^2(Inf)}{d\left(\frac{H}{w}\right)^2} > 0$$

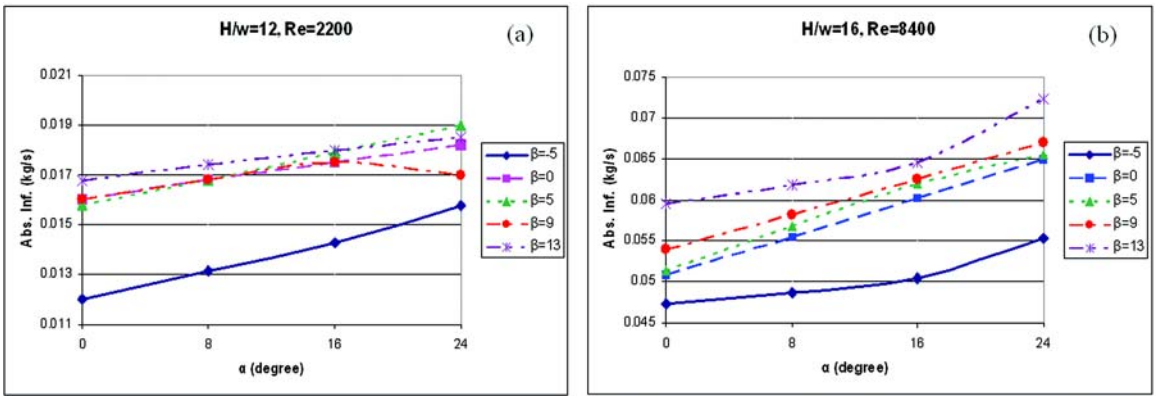

Figure 8 *Effect of offset angle.*

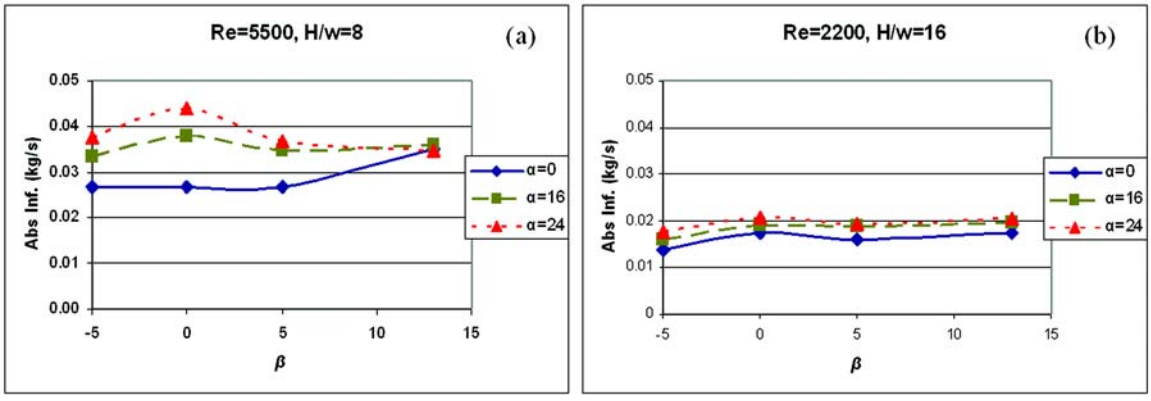

Figure 9 *Effect of throw angle.*

In some other cases such as the case that $\beta = 13°$ and Re=2,200 (Figure 10c), we will see an increasing pattern but with a declining growth in infiltration when *H/w* increases, as seen below:

$$\frac{d(Inf)}{d\left(\frac{H}{w}\right)} > 0, \quad \frac{d^2(Inf)}{d\left(\frac{H}{w}\right)^2} < 0$$

On the other hand, Figure 10d shows a case that gathers all the above patterns when offset angle varies. Therefore, the offset angle is one of the important factors that should be considered when determining opening height.

As mentioned previously, by using tracer gas technique we can also measure the total mass flow rate of a display case at the RAG, to calculate the absolute infiltration flow rate from Equation 1. Figure 11a depicts only the concentrations of CO_2 in the DAG and RAG which are required in Equation 8. The measurements were taken at an environmentally-controlled laboratory in Refrigeration & Thermal Test Center of Southern California Edison. The condition of the test laboratory was set to 75 F and 55% R.H. for ambient (laboratory space), and 30 F for temperature of the DAG. Figure 11b presents the volumetric flow rate at the RAG that can be found from Equation 8. In the first 200 seconds of the test it was allowed the air and tracer gas flow inside the system and the laboratory to reach steady state. The slight increase of the flow rate with time in Figure 11b is due to the relatively rapid increase and accumulation of tracer gas within the small space of laboratory. The average calculated flow rate was about 415 cfm (0.196 m^3/s) which is relatively acceptable with a conventional handheld velometer with modest accuracy that reported about 452 cfm (0.213 m^3/s).

The uncertainty in measuring the total air flow rate, associated with adding the tracer gas mass is (Amin et al., 2008-a):

$$\frac{\dot{m}_{RAG}}{\dot{m}_{air}} - 1 = \frac{C_{RAG}}{1 - C_{RAG}} \tag{11}$$

One may anticipate that by increasing the mass of released tracer gas, the divergence of the measured flow from the actual air flow rate be increased. During our tests, the C_{RAG} was usually below 2% (with uncertainty about 2.1%), but even with increase of this value to 3% (which rarely occurs), the divergence will be only 3.1%. The uncertainty corresponding to the results of Figure 11 is about 1.75%.

So far, the presented results have been for the cases with no food products on shelves. To take into account the effect of

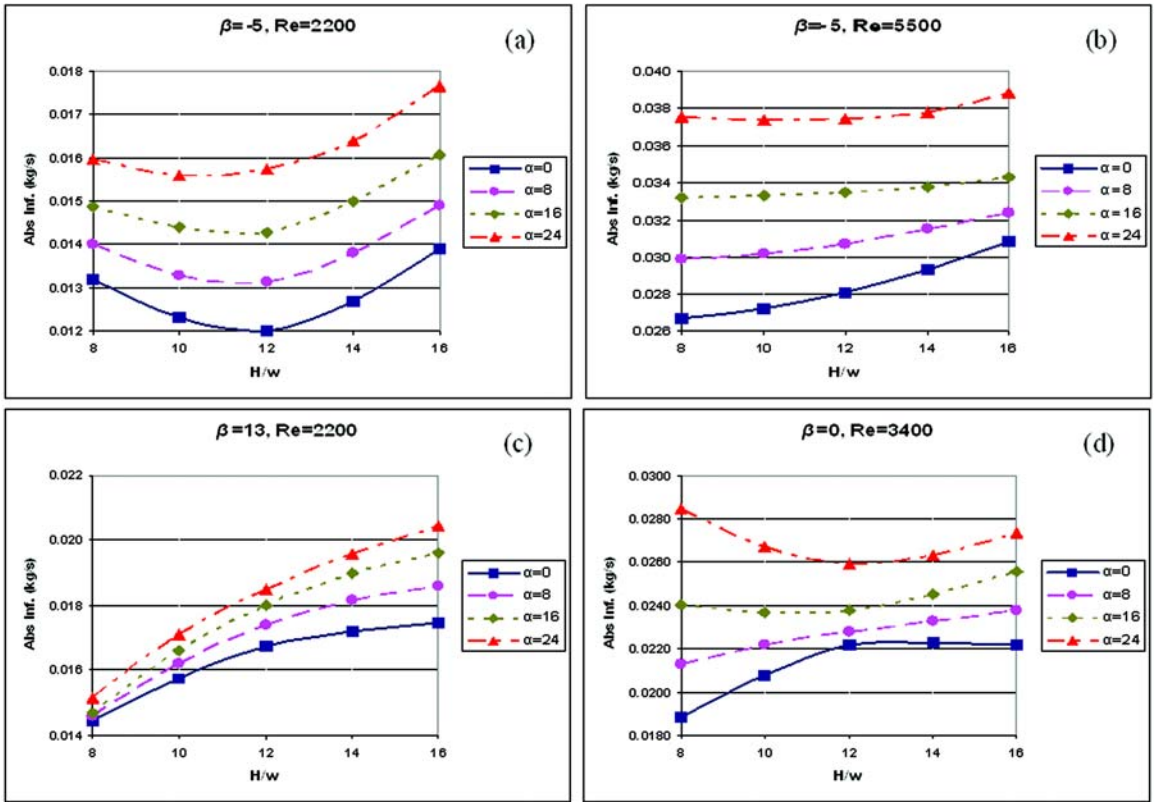

Figure 10 *Effect of opening height.*

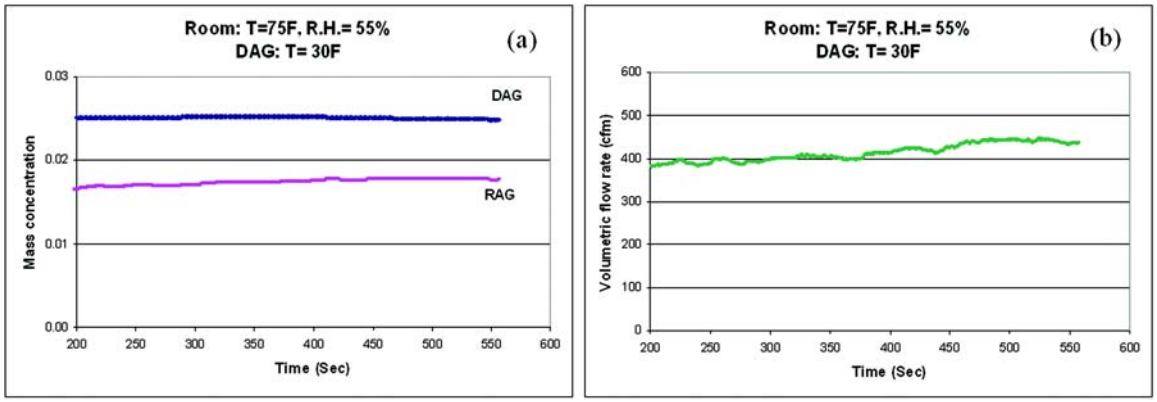

Figure 11 *(a) Mass concentration of CO_2 and (b) total (RAG) volumetric flow rate.*

food product levels, the tests were repeated for a few test cases with several food levels. Equation 12 estimates the shelves food level (x) on the infiltration in the form of a correction factor (Z).

$$Z = 0.55(1 - R)[Z_2 - Z_1] + Z_1 \tag{12}$$

where,

$$Z_1 = \frac{\alpha}{24}(-1.27x^2 + 1.11x) + 0.362x^2 - 0.52x + 1 \tag{13}$$

$$Z_2 = \frac{\alpha}{24}(-0.033x^2 - 0.646x) - 0.259x^2 - 0.64x + 1 \tag{14}$$

$$0 \le x \le 1, \text{ and } R = \frac{\dot{m}_{DAG}}{\dot{m}_{RAG}}$$

Therefore, the corrected infiltrations can be stated as:

$$\begin{aligned}&(\text{Absolute Infiltration Rate})_{\text{with\_food}} \\ &= (\text{Absolute Infiltration Rate})_{\text{without\_food}} \cdot Z(x, \alpha, R)\end{aligned} \tag{15}$$

or

$$(\text{N.I.R})_{\text{with\_food}} = (\text{N.I.R.})_{\text{without\_food}} \cdot Z(x, \alpha, R) \tag{16}$$

CONCLUSION

Finding the effect of several geometrical variables and air speed on the infiltration rate of open refrigerated vertical display cases was of the interest of this study. Instead of testing each individual configuration by constructing a new display case or retrofitting existing display cases, which all can cost a lot, a simulator has been designed and constructed so that it can easily meet all those variables. The results of all permutations of variables have shown that infiltration is a strong function of Reynolds number, offset angle, throws angle and opening height. With increase of Reynolds number, the absolute infiltration rate increases almost linearly; however, the non-dimensional infiltration rate decreases implying that although the air curtains with higher momentum cause greater entrainments, they are not fortunately as efficient as lower-speed jets in entraining the ambient air. Further investigations have shown that with increase of offset angle, the infiltration increases almost linearly. Within the range of the tested throw angle, β =-5° produces the least infiltration rate, and depending on the magnitude of other variables such as α, Re and *H/w*, different trends may be observed for the infiltration. Similarly, the variation of infiltration with respect to *H/w* is contingent to the other variables.

In this work, a new accurate technique for measuring the total mass flow rate of the display case was introduced as well. This method is based on an added tracer gas in a confined control volume within a duct.

FUTURE WORK

As mentioned before, a series of studies have been conducted to study the effect of offset angle (α), throw angle (β), Reynolds number (Re), and height-to-width ratio (*H/w*) on the infiltration rate of the ORVDCs. Our future investigation will be devoted to other values of $R = \frac{\dot{m}_{DAG}}{\dot{m}_{RAG}}$, and finally to the overall comparison between infiltrations of all values of R including zero value.

ACKNOWLEDGMENT

This work is sponsored in part by the US Department of Energy (under contract DE-AC05-00OR22725 with UT-Battelle, LLC**.**), California Energy Commission and Southern California Edison Co. The authors would like to thank Mr. Ramin Faramarzi, the manager of Refrigeration and Thermal Test Center at Southern California Edison Co. for his long time

support. The authors also appreciate Mr. Justin Zuehlke for helping editing this manuscript.

NOMENCLATURE

Amb	=	ambient
Abs	=	absolute
BP	=	back panel (flow)
C	=	mass concentration of tracer gas
DAG	=	discharge air grille
H	=	vertical distance between DAG and RAG
Inf	=	infiltrated
Inj	=	injected
$\dot{m}$	=	mass flow rate
N.I.R.	=	non-dimensional infiltration rate
ORVDC	=	open refrigerated vertical display case
R	=	DAG to DAG volumetric flow rates ratio
RAG	=	return air grille
Re	=	Reynolds number [$=(V w_{DAG})/\upsilon$]
T	=	average temperature
tot	=	total
trac	=	tracer gas
x	=	food level on shelves ($0 \le x \le 1$)
x-y-z	=	coordinate system
Y	=	horizontal distance between DAG and RAG
V	=	average velocity at the DAG
w	=	width of the DAG or RAG
Z	=	Food level-related correction factor for infiltration rate
α	=	offset angle (atan[Y/H])
β	=	air curtain jet throw angle at the DAG discharge
η	=	thermal entrainment
υ	=	kinematic viscosity

REFERENCES

ACGIH. 1971. Carbon dioxide. Documentation of the threshold limit values for substances in workroom air. *American Conference of Governmental Industrial Hygienists*, Cincinnati, OH, 3rd edition, pp. 39.

Amin, M., Dabiri, D., and Navaz, K. 2008a. Tracer Gas Technique: a New Approach for Steady State Infiltration Rate Measurement of Open Refrigerated Display Cases. *Journal of Food Engineering*. (in press)

Amin, M., Navaz, H.K., Dabiri, D., and Faramarzi. R. 2008b. Air curtains of open refrigerated display cases revisited: a new technique for infiltration rate measurements. *10th International Conference on Advanced Computational Methods and Experimental Measurements in Heat Transfer, Maribor, Slovenia, July 9-11*.

California Energy Commission (CEC) & Southern California Edison (SCE) Co. 2003. *Private communications*.

Faramarzi, R., Amin, M., Navaz, H.K., Dabiri, D., Rauss, M., and Sarhadian, R. submitted 2008. Air curtain stability and effectiveness in open vertical display cases. Report prepared by Southern California Edison Co. for California Energy Commission.

Howell, R.H., and Adams, P.A. 1991. Effects of indoor space conditions on refrigerated display case performance. *ASHRAE Research Project 596-RP.* Department of Mechanical Engineering, University of South Florida, Tampa.

IDLH Documentation. 2007. Carbon dioxide. *National Institute for Occupational Safety and Health*.

McWilliams, J. 2002. Review of Airflow Measurement Techniques. LBNL-49747.

Navaz, H.K., Faramarzi, R., Dabiri, D., Gharib, M. and Modarress, D. 2002. The application of advanced methods in analyzing the performance of the air curtain in a refrigerated display case. *ASME Journal of Fluid Engineering*, 124: 756-764.

Navaz, H.K., Amin, M., Dabiri, D., and Faramarzi, R. 2005a. Past, Present, and Future Research Toward Air Curtain Performance Optimization. *ASHRAE Transactions*, 111 (1): 1083-1088.

Navaz, H.K., Henderson, B.S., Faramarzi, R., Pourmovahed, A., and Taugwalder, F. 2005b. Jet entrainment rate in air curtain of open refrigerated display cases. *International Journal of Refrigeration*, 28(2): 267-275.

Rigot, G. 1990. Meubles et vitrines frigorifiques, Pyc ed, Paris, France.